Supplementary Materials

A Chemical-Enhanced System for CRISPR-Based Nucleic Acid Detection

Zihan Li[1,2,†], Wenchang Zhao[1,2,†], Shixin Ma[1,2,†], Zexu Li[1,2], Yingjia Yao[1,2], Teng Fei[1,2,*]

[1]College of Life and Health Sciences, Northeastern University, Shenyang 110819, People's Republic of China;
[2]Key Laboratory of Data Analytics and Optimization for Smart Industry (Northeastern University), Ministry of Education, Shenyang 110819, People's Republic of China

[†]These authors contributed equally to this work
*Corresponding author: feiteng@mail.neu.edu.cn

This document includes:

Supplementary Materials and Methods

Constructs and reagents

The coding regions of LwaCas13a (*Leptotrichia wadeii* Cas13a)(Abudayyeh et al. 2017), AsCas12a (*Acidaminococcus sp.* Cas12a)(Li et al. 2018) and LbCas12a (*Lachnospiraceae bacterium* Cas12a)(Li et al. 2018) were inserted into pET28a expression vector between BamHI and XhoI restriction enzyme sites for prokaryotic expression and purification of these proteins. N gene fragments (two different regions: #1 and #2) from SARS-CoV-2 viral genome were inserted into pHAGE-EF1α-puro vector between BamHI and KpnI restriction enzyme sites for SARS-CoV-2 pseudovirus detection. Oligonucleotides used in this study (Table S2) were synthesized from HuaGene Biotech (Shanghai, China), Synbio Technologies (Suzhou, China) and GENEWIZ (Suzhou, China). Detailed information about reagents and instruments, including the commercial vendors and item numbers, is provided in Table S3.

Nucleic acid preparation

For preparation of DNA templates of SARS-CoV-2 ORF1ab, N and S genes, PCR amplification was performed by indicated primers with the forward primer containing an appended T7 promoter sequence using the template prepared through annealing of two synthetic oligonucleotides (Table S2). For preparation of RNA templates, the in vitro transcription was performed with T7 promoter-inclusive DNA templates. Briefly, the in vitro transcription (IVT) system consisted of 4 μL 10x Transcription Buffer, 3.125 mM rNTPs, 50U T7 RNA Polymerase (Lucigen), 1 μL RNase Inhibitor and 50~100 ng DNA template, and the total reaction volume was 40 μL. After thorough mixing, the reaction system was incubated at 37°C for 1~2 hour (h). For preparation of crRNAs, the DNA oligonucleotide containing reverse complementary sequence of crRNA was annealed to an oligo (T7-F) with T7 promoter sequence to form a partial duplex DNA template for IVT. Then crRNAs were in vitro transcribed using the same IVT reaction system as described above. RNA templates and crRNAs were purified by RNA Clean & Concentrator-5 Kit (Zymo research), and quantified by the high sensitivity RNA Qubit fluorometer (Thermo Fisher).

Cas protein expression and purification

Cas protein expression plasmids (pET28a-AsCas12a, pET28a-LbCas12a and pET28a-LwaCas13a) were transformed into *Escherichia coli.* Rosseta™ 2(DE3)pLySs competent cells. After transformation, cells were plated on kanamycin and chloramphenicol positive Luria-Bertani (LB) agar plate, and incubated for 16 h at 37°C. Pick up one colony from the plate, inoculate in 5 mL liquid LB medium supplemented with kanamycin and chloramphenicol, and put the starter culture on a shaker at 37°C overnight. 5 mL of starter culture was used to inoculate 1L of LB media supplemented with antibiotics and shaked at 37°C with 300 r.p.m. Cultures were allowed to grow until OD_{600} reached 0.4~0.6, and then cooled down for 30 minute (min) at 4°C. Add isopropyl β-D-thiogalactoside (IPTG) to a final concentration of 0.5 mM to induce protein expression for 14-16 h at 300 r.p.m. in a pre-chilled 20°C shaker. After induction, the cells were harvested by centrifugation (5000 g, 4°C, 10 min) for later purification and stored at -80°C.

Protein purification procedures were performed at 4°C. Cell pellet was resuspended in 15 mL of lysis buffer (20 mM Tris-HCl (pH 8.0), 500 mM NaCl, 1 mM DTT, 5% glycerol, 1 mM PMSF, 1 mg/mL lysozyme). The cell lysate was then sonicated by the sonicator with the following parameters: sonication (φ6, power 40%) for 1 second on and 2 seconds off with a total sonication time of 15 min. The sonicated sample was then centrifuged at 14000 r.p.m. for 10 min at 4°C and the supernatant was mixed with an equal volume of equilibration/wash buffer (50 mM sodium phosphate, 300 mM sodium chloride, 10 mM imidazole; pH 7.4). Since the recombinant Cas protein contains His-tag, HisPur™ Cobalt Resin (Thermo Fisher, #89964) was utilized to pull-down the protein. Washed protein extract was mixed with the prepared cobalt resin on end-over-end rotator for 30 min at 4°C followed by washing of the protein-bound cobalt resin twice in equilibration/wash buffer. Elute bound His tagged protein using elution buffer (50 mM sodium phosphate, 300 mM sodium chloride, 150 mM imidazole; pH 7.4) twice. Zeba™ Spin Desalting Columns (Thermo Fisher, #89890) was used to desalt protein, and ~2 mL protein could be collected after centrifuging at 850 g for 2 min. Mix the protein with 10 mL Storage Buffer (600 mM NaCl, 50 mM Tris-HCl (pH 7.5), 5% glycerol, 2 mM DTT), and transfer the mix into Amicon® Ultra-15 Centrifugal Filter Devices (Millipore, #UFC905008) to concentrate the protein and exchange the storage buffer as well. The concentration of purified proteins was quantified by BCA protein assay kit (Meilunbio, #MA0082). SDS-PAGE analysis was performed with samples collected after different purification steps and the results were visualized by Coomassie Blue staining. Purified protein was stored at -80°C as 10 μL aliquots at a concentration of 2 mg/mL.

CRISPR detection assay

CRISPR-LwaCas13a system was used for RNA detection. The standard LwaCas13a-based detection assay was performed at 37°C with 1x CutSmart buffer, 100 nM LwaCas13a protein, 100 nM crRNA, 250 nM RNA reporter and 1 μL of nucleic acid target in a 20 μL reaction system. For DNA detection system, CRISPR-AsCas12a and CRISPR-LbCas12a systems were applied. The standard reaction systems of Cas12a-based nucleic acid detection consisted of 1x CutSmart buffer, 50 nM AsCas12a protein or LbCas12a protein, 50 nM crRNA, 250 nM DNA reporter, and 1 μL of nucleic acid target or amplification products in a final volume of 20 μL at 37°C for 1 h. For the optimization of the detection systems, indicated amount of components and specified chemicals were added to the detection systems. For the stoichiometry of Cas protein/crRNA, we quantified the mass of Cas protein using BCA protein assay kit and calculated the molar mass of each crRNA by their specific nucleic acid identity. Thus, the molecular ratio of Cas protein/crRNA in reaction system could be determined.

Fluorescence readout

The CRISPR-LwaCas13a and CRISPR-AsCas12a (LbCas12a) fluorescence detection assays were performed by using fluorophore-quencher (FQ) reporters involving a short single-stranded (ss) RNA or DNA oligonucleotide, respectively. Both of the ssRNA and ssDNA FQ reporters were composed of a 6-FAM fluorophore on 5 terminal and a BHQ1 quencher on 3 terminal

(ssRNA FQ reporter: 5′ -/6-FAM/UUUUUU/BHQ1/-3′; ssDNA FQ reporter: 5′ -/6-FAM/TTATT/BHQ1/-3′). For LwaCas13a-based assay, the detection system consisted of 100 nM LwaCas13a, 100 nM crRNA, 250 mM ssRNA fluorescent reporter, 1x CutSmart Buffer and 1 μL nucleic acid target in a 20 μL reaction system. For AsCas12a- and LbCas12a-based assays, the detection system contained 50 nM AsCas12a or LbCas12a protein, 50 nM crRNA, 250 nM ssDNA fluorescence reporter, 1x CutSmart Buffer and 1 μL DNA target or amplification products. Fluorescence signal was dynamically measured by QuantStudio™ 5 Real-Time PCR System (Thermo Fisher). Background-subtracted signals for each monitoring points were further normalized by subtraction of its initial value to make comparison between different conditions (arbitrary unit, a.u.) for the analysis. Visual detection was accomplished by imaging the tubes through E-Gel™ Safe Imager™ Real-Time Transilluminator (Thermo Fisher).

Lateral flow readout

For lateral flow strip assays, the AsCas12a-based detection system was assembled as described above except that the fluorescence reporter was replaced with the biotin-labeled reporter. Lateral flow cleavage reporter (5′ -/6-FAM/TTATTATT/Biotin/-3′) was added to the reaction at a final concentration of 250 nM in 20 μL reaction volume along with the 1 μL RT(reverse transcription)-LAMP product, and incubate the reaction at 37°C for 1 h. After completion of the incubation, add 80 μL HybriDetect Assay Buffer into the reaction tube. A lateral flow strip (Milenia Biotec GmbH, # MGHD 1) was placed to the reaction tube and incubated for approximately 3~5 min, and the result was visualized directly. The negative result is indicated by one primary band at the control line (C), and significant band in test line (T) represents positive result.

LAMP assay

For detection of SARS-CoV-2 RNA, RT-LAMP reactions were performed with caution on a dedicated clean bench using filter tips to prevent sample contamination. One-step RT-LAMP mix was assembled with 1 μL 10x isothermal amplification buffer, 1.4 mM of dNTPs, 6.5 mM $MgSO_4$, 3.2 U Bst 2.0 (NEB, #M0538S), 3 U WarmStart RTx Reverse Transcriptase (NEB, #M0380S), 0.2 μM F3/B3 primers, 1.6 μM FIP/BIP primers, 0.8 μM LF/LB primers, and 1 μL of RNA template in a 10 μL volume, and then incubated at 62°C for 15~30 min. Primers for LAMP are listed in Table S2. The heat inactivation (80°C for 20 min) of LAMP product was performed to reduce the background signal before proceeding to CRISPR detection assays. Quantitative real-time PCR was conducted using non-specific DNA-binding dye EvaGreen (Biotium, #31000) to quantitate the total amount of amplification products. EvaGreen-derived fluorescence signal was normalized by subtraction of initial value to make comparison between different conditions. For evaluation of the target specificity of LAMP reactions, amplification products were purified by PCR Purification Kit (Thermo Fisher, #K0702), and followed by fluorescence detection with AsCas12a system. The purified products might be diluted to an appropriate concentration to make sure the detection signal fell into the effective detection range.

RPA assay

RPA assays were set up using commercial RPA kit (TwistDx). One step RT-RPA reaction system was composed of 9 μL of RPA solution (primer-free rehydration buffer), 224 mM of MgOAc, 40 U of ProtoScript II Reverse Transcriptase (NEB, #M0368S), 0.5 μM of forward primer, 0.5 μM of reverse primer and UltraPure water to a total volume of 16 μL. Primers for RPA are listed in Table S2. The mixture was incubated at 40°C for 30 min, followed by heat inactivation for 20 min at 80°C. Total amount of amplification product was quantified by quantitative real-time PCR using EvaGreen dye, and specific target amplification was determined by AsCas12a-based CRISPR detection after purification using PCR Purification Kit.

qRT-PCR assay

Standard SARS-CoV-2 Reference RNA material (GBW(E)091089, National Institute of Metrology, China) was diluted to different concentrations. qRT-PCR assay was performed using commercial Novel Coronavirus (2019-nCoV) Dual Probes qRT-PCR Kit (Beyotime, Cat.D8006S). In brief, mix 17.5μL reaction buffer, 2.5 μL enzyme mix and 5 μL different concentration of template RNA as a 25 μL reaction system. Set up the qRT-PCR program in QuantStudio™ 5 Real-Time PCR System (Thermo Fisher) as follows: 20 min 50°C for reverse transcription, 2 min 95°C for pre-denaturation, 45 cycles of 15 sec 95°C degeneration and 20 sec 60°C annealing/elongation. The concentration of input RNA can be correlated with corresponsive Ct values.

Pseudovirus production and detection

HEK293FT cells were employed to pack the SARS-CoV-2 pseudoviral particles. Cells were cultured with DMEM medium supplemented with 10% fetal bovine serum. DNA Transfection was performed in 6-well plates by Lipofectamine™ 2000 Transfection Reagent with a mix of 1.5 μg pHAGE-EF1α-puro plasmid carrying SARS-CoV-2 N gene fragment (#1 and #2), 0.75 μg pCMVR8.74, and 0.5 μg pMD2.G. The viral particle-containing supernatant was harvested at 48 h post transfection and centrifuged at 3000 r.p.m for 5 min to remove the cell debris. Aliquot and store the virus supernatant at -80°C before use. For virus titration, a commercial Lentivirus Titer Kit was used (Abm, #LV900). Briefly, 1μL virus supernatant was lysed in 9μL Virus Lysis Buffer for 3 min at room temperature. Quantitative Reverse Transcription PCR (qRT-PCR) was performed with specified primer set to quantify the viral particles. The titer of virus can be calculated from online lentiviral titer calculator which is provided by Abm at http://www.abmgood.com/High-Titer-Lentivirus-Calculation.html. To simulate the actual application, viral particles were firstly transferred into the Viral Transport Media (VTM) of Sample Collection Kit (BEAVER, #43903) to a final volume of 1 mL as a mimic of nasopharyngeal swab collected sample. Take out 100 μL solution for RNA extraction by UNIQ-10 Column Trizol Total RNA Isolation kit (Sangon, #B511321-0100), and elute the RNA by 50 μL UltraPure H_2O. RT-LAMP was performed with 1 μL extracted RNA as template followed by AsCas12a-based detection in the absence or presence of L-proline.

Statistical analysis

Statistic significances were calculated by GraphPad Prism 8.4.0 and all the data were shown as mean ± s.d. The two-way ANOVA with Sidak's multiple comparisons test was used to compare differences between groups. Statistical significance was determined by an unpaired two-tailed t-test. Asterisks indicate $^{**}p < 0.01$, $^{***}p < 0.001$, $^{****}p < 0.0001$.

Supplementary Discussion

In this study, we have explicitly revealed several basic features affecting the efficiency and sensitivity of different CRISPR detection systems. We further systematically evaluated several chemical additives for their effects on detection performance during either CRISPR detection phase or target amplification phase. By adding L-proline into the two-step CRISPR detection systems, we established an enhanced CRISPR detection toolkit named CECRID that exhibits improved system stability and detection power as evidenced using SARS-CoV-2 contrived gene template assays and pseudoviral particle testing. In addition, we also discussed some tips and procedures such as introducing nested amplification primers and reverse transcriptase inactivation towards improved CRISPR detection. These results will help to provide better CRISPR-based diagnostic solutions and expedite their practical applications for POCT purpose.

Chemical approaches have been adopted to modulate the activity of CRISPR/Cas system from several aspects: 1) chemical substance (e.g., 4-hydroxytamoxifen) can be used to achieve spatiotemporal control for Cas protein activity (Liu et al. 2016; Maji et al. 2017); 2) special chemical modifications are introduced into gRNA nucleotides for better stability, less off-target pairing or weaker immunogenicity (Yin et al. 2017); 3) chemical engineering is applied to facilitate non-viral delivery of Cas protein:gRNA ribonucleoprotein complex into the cells (Zhang et al. 2021). All the above chemical engineering strategies are implemented to enhance the in vivo performance of CRISPR apparatus. For CRISPR-based in vitro application such as trans-cleavage-mediated nucleic acid detection, using chemical substance to boost CRISPR detection activity has not been thoroughly investigated. In contrast, several previous studies have tested the effects of chemical additives on in vitro target amplification by classic PCR. Some typical chemicals such as betaine, DMSO, BSA, dithiothreitol (DTT), and glycerol have been shown to improve the product specificity and/or yield during PCR amplification, especially for the difficult reactions with long or GC-rich template (Henke et al. 1997; Jensen et al. 2010; Nagai et al. 1998; Ralser et al. 2006; Varadharajan and Parani 2021). In addition, betaine was also reported to reduce non-specific product and enhance the amplification efficiency for isothermal RPA reaction (Luo et al. 2019). However, betaine addition in LAMP reaction rather play an inhibitory role for target amplification, possibly due to the molecular barrier function of betaine to hinder intermolecular hybridization (Ma et al. 2017). Joung et al recently established a one-pot SHERLOCK assay by combining LAMP-mediated target amplification and Cas12b-based CRISPR detection for SARS-CoV-2 viral detection (Joung et al. 2020). They found that addition of either glycine or taurine into the one-pot reaction mix exhibited ~2-fold enhancement of the final detection signal (Joung et al. 2020). However, these assays were only performed under one condition with specified primer/crRNA set, and the enzymatic constituents are quite complicated (including reverse transcriptase, DNA polymerase and Cas12b). Thus, it is still obscure to conclude whether the roles of these chemical additives are general for such type of reaction and on which step or component they exert the effect if any. Our work here systematically evaluated several commonly used chemical additives for their effects on either trans-cleavage-mediated CRISPR detection or LAMP/RPA-based

isothermal target amplification, and identified a previously unrecognized chemical L-proline as a consistent chemical enhancer for these reactions.

General PCR enhancers such as betaine and DMSO are considered to play their roles by assisting double stranded DNA unwinding, lowering the melting temperature, reducing the formation of unwanted secondary structure between DNA strands, and facilitating primer annealing and extension (Henke et al. 1997; Jensen et al. 2010; Ralser et al. 2006; Varadharajan and Parani 2021). In contrast, BSA is not used as a typical PCR enhancer except for some difficult scenarios such as amplification from soil or plant samples that contain PCR inhibitor substance within the template (Farell and Alexandre 2012; Kageyama et al. 2003; Plante et al. 2011). BSA may bind to and neutralize the inhibitor as a blocking reagent, thereby promoting the amplification. BSA is usually regarded as a protein stabilizer by increasing the thermal stability and half-life of the enzymes during some typical molecular cloning-related reactions such as restriction enzyme digestion of DNA. In addition, human serum albumin or recombinant albumin was often included as a stabilizer in the formula for biological and medical reagents such as cytokine/hormone peptide and vaccine (Marth and Kleinhappl 2001; Tarelli et al. 1998). Consistently, here we did not conclude a definite effect of BSA on isothermal amplification reactions despite some beneficial role for RPA assay with single specified primer/crRNA set. However, we did reveal a dramatic enhancement effect of BSA on CRISPR-based trans-cleavage reaction, suggesting that BSA should serve as a necessary component in CRISPR detection buffer. We posit that BSA may achieve this enhancement function through some or all of the following mechanisms: 1) stabilize Cas protein and other macromolecules in the reaction; 2) neutralize unknown inhibitory substance within the system especially from protein purification or nucleic acid preparation; 3) facilitate proper Cas protein refolding by modulating the solvent property; and 4) reduce the absorbance of reaction components on the test tube surface as a coating reagent.

L-proline is one of the most abundant molecules in cells and frequently used amino acids in natural proteins (Morita et al. 2003). Proline residue plays an important role for protein folding via controlling the cis/trans isomerization of peptide bonds (Zosel et al. 2018). Pathogenic proline substitution is related to misfolding and aberrant aggregation of key protein presenilin 1 in Alzheimer's disease (Ben-Gedalya et al. 2015). In addition, proline-rich peptides were shown to possess immunomodulatory and neuroprotective properties against neurodegenerative diseases (Gladkevich et al. 2007). L-proline monomer can serve as natural osmoprotectant and cryoprotectant for cells exposed to osmotic and cold stresses possibly by preserving membrane integrity, stabilizing proteins and facilitating protein folding (Bolli et al. 2010; Morita et al. 2003). Accordingly, L-proline was chosen as a stabilizer for liquid intravenous immunoglobulin (IVIG) products (Berger 2011; Hagan et al. 2012). Moreover, L-proline can serve as an efficient catalyst for several types of reactions in organic synthesis (Rao et al. 2013; Tanimoro et al. 2012; Yang et al. 2008). Here we found that L-proline, among other tested chemical additives, exhibits the most consistent effect in reinforcing the detection power during both the target amplification phase and CRISPR signal detection phase. Addition of L-proline significantly

enhances the specific target amplification for LAMP and RPA reactions, which may be attributed to the multifaceted properties of L-proline such as stabilizing protein enzyme, assisting protein refolding, modulating the molecular interaction and creating favorable solvent environment. Interestingly, the effect of L-proline on CRISPR-mediated trans-cleavage depends on the buffer composition and even the buffer batch. Unlike BSA, which is a bona fide enhancer for CRISPR cleavage reaction, L-proline does not directly promote the CRISPR detection signal in less-favored buffers (e.g. BSA-null buffers) or certain batches of well-kept favored buffers (e.g. CutSmart buffer). Rather, L-proline displays an enhancer effect in the buffers when BSA is not in optimal conditions or the Cas protein enzyme is partially denatured. These results indicated that L-proline here may act as a system stabilizer to protect essential buffer component BSA and/or Cas enzyme from environmental stresses, thereby safeguarding their activities under suboptimal conditions. This notion is further supported by our data and previous reports showing that proline can prevent the aggregation of BSA and other proteins resulted from heat- or chemical-induced denaturation (Dasgupta and Kishore 2017; Kumar et al. 1998). Considering the complexity of the CRISPR reaction mix, the batch difference of reagent quality in applicable test kit is not only confined to the buffer system, but also expands to Cas enzymes, gRNAs and reporters throughout the whole manufacturing, transportation, storage and on-site testing processes. The inclusion of L-proline in the CRISPR detection mix provide an additional safety layer to secure the detection power and/or enhance the performance. More importantly, when CRISPR detection is conjugated with LAMP/RPA-based target amplification, L-proline as a system enhancer is compatible for both phases which simplifies the whole detection pipeline.

Supplementary References

Abudayyeh, O.O., Gootenberg, J.S., Essletzbichler, P., Han, S., Joung, J., Belanto, J.J., Verdine, V., Cox, D.B.T., Kellner, M.J., Regev, A., Lander, E.S., Voytas, D.F., Ting, A.Y., Zhang, F., 2017. RNA targeting with CRISPR-Cas13. Nature 550(7675), 280-284.

Ben-Gedalya, T., Moll, L., Bejerano-Sagie, M., Frere, S., Cabral, W.A., Friedmann-Morvinski, D., Slutsky, I., Burstyn-Cohen, T., Marini, J.C., Cohen, E., 2015. Alzheimer's disease-causing proline substitutions lead to presenilin 1 aggregation and malfunction. The EMBO journal 34(22), 2820-2839.

Berger, M., 2011. L-proline-stabilized human IgG: Privigen(R) 10% for intravenous use and Hizentra(R) 20% for subcutaneous use. Immunotherapy 3(2), 163-176.

Bolli, R., Woodtli, K., Bartschi, M., Hofferer, L., Lerch, P., 2010. L-Proline reduces IgG dimer content and enhances the stability of intravenous immunoglobulin (IVIG) solutions. Biologicals : journal of the International Association of Biological Standardization 38(1), 150-157.

Broughton, J.P., Deng, X., Yu, G., Fasching, C.L., Servellita, V., Singh, J., Miao, X., Streithorst, J.A., Granados, A., Sotomayor-Gonzalez, A., Zorn, K., Gopez, A., Hsu, E., Gu, W., Miller, S., Pan, C.Y., Guevara, H., Wadford, D.A., Chen, J.S., Chiu, C.Y., 2020. CRISPR-Cas12-based detection of SARS-CoV-2. Nature biotechnology 38(7), 870-874.

Dasgupta, M., Kishore, N., 2017. Selective inhibition of aggregation/fibrillation of bovine serum albumin by osmolytes: Mechanistic and energetics insights. PloS one 12(2), e0172208.

Farell, E.M., Alexandre, G., 2012. Bovine serum albumin further enhances the effects of organic solvents on increased yield of polymerase chain reaction of GC-rich templates. BMC research notes 5, 257.

Gladkevich, A., Bosker, F., Korf, J., Yenkoyan, K., Vahradyan, H., Aghajanov, M., 2007. Proline-rich polypeptides in Alzheimer's disease and neurodegenerative disorders -- therapeutic potential or a mirage? Progress in neuro-psychopharmacology & biological psychiatry 31(7), 1347-1355.

Hagan, J.B., Wasserman, R.L., Baggish, J.S., Spycher, M.O., Berger, M., Shashi, V., Lohrmann, E., Sullivan, K.E., 2012. Safety of L-proline as a stabilizer for immunoglobulin products. Expert review of clinical immunology 8(2), 169-178.

Henke, W., Herdel, K., Jung, K., Schnorr, D., Loening, S.A., 1997. Betaine improves the PCR amplification of GC-rich DNA sequences. Nucleic acids research 25(19), 3957-3958.

Jensen, M.A., Fukushima, M., Davis, R.W., 2010. DMSO and betaine greatly improve amplification of GC-rich constructs in de novo synthesis. PloS one 5(6), e11024.

Joung, J., Ladha, A., Saito, M., Kim, N.G., Woolley, A.E., Segel, M., Barretto, R.P.J., Ranu, A., Macrae, R.K., Faure, G., Ioannidi, E.I., Krajeski, R.N., Bruneau, R., Huang, M.W., Yu, X.G., Li, J.Z., Walker, B.D., Hung, D.T., Greninger, A.L., Jerome, K.R., Gootenberg, J.S., Abudayyeh, O.O.,

Zhang, F., 2020. Detection of SARS-CoV-2 with SHERLOCK One-Pot Testing. The New England journal of medicine 383(15), 1492-1494.

Kageyama, K., Komatsu, T., Suga, H., 2003. Refined PCR protocol for detection of plant pathogens in soil. Journal of General Plant Pathology 69(3), 153-160.

Kumar, T.K., Samuel, D., Jayaraman, G., Srimathi, T., Yu, C., 1998. The role of proline in the prevention of aggregation during protein folding in vitro. Biochemistry and molecular biology international 46(3), 509-517.

Li, S.Y., Cheng, Q.X., Liu, J.K., Nie, X.Q., Zhao, G.P., Wang, J., 2018. CRISPR-Cas12a has both cis- and trans-cleavage activities on single-stranded DNA. Cell research 28(4), 491-493.

Liu, K.I., Ramli, M.N., Woo, C.W., Wang, Y., Zhao, T., Zhang, X., Yim, G.R., Chong, B.Y., Gowher, A., Chua, M.Z., Jung, J., Lee, J.H., Tan, M.H., 2016. A chemical-inducible CRISPR-Cas9 system for rapid control of genome editing. Nature chemical biology 12(11), 980-987.

Luo, G.C., Yi, T.T., Jiang, B., Guo, X.L., Zhang, G.Y., 2019. Betaine-assisted recombinase polymerase assay with enhanced specificity. Analytical biochemistry 575, 36-39.

Ma, C., Wang, Y., Zhang, P., Shi, C., 2017. Accelerated isothermal nucleic acid amplification in betaine-free reaction. Analytical biochemistry 530, 1-4.

Maji, B., Moore, C.L., Zetsche, B., Volz, S.E., Zhang, F., Shoulders, M.D., Choudhary, A., 2017. Multidimensional chemical control of CRISPR-Cas9. Nature chemical biology 13(1), 9-11.

Marth, E., Kleinhappl, B., 2001. Albumin is a necessary stabilizer of TBE-vaccine to avoid fever in children after vaccination. Vaccine 20(3-4), 532-537.

Morita, Y., Nakamori, S., Takagi, H., 2003. L-proline accumulation and freeze tolerance of Saccharomyces cerevisiae are caused by a mutation in the PRO1 gene encoding gamma-glutamyl kinase. Applied and environmental microbiology 69(1), 212-219.

Nagai, M., Yoshida, A., Sato, N., 1998. Additive effects of bovine serum albumin, dithiothreitol, and glycerol on PCR. Biochemistry and molecular biology international 44(1), 157-163.

Plante, D., Belanger, G., Leblanc, D., Ward, P., Houde, A., Trottier, Y.L., 2011. The use of bovine serum albumin to improve the RT-qPCR detection of foodborne viruses rinsed from vegetable surfaces. Letters in applied microbiology 52(3), 239-244.

Ralser, M., Querfurth, R., Warnatz, H.J., Lehrach, H., Yaspo, M.L., Krobitsch, S., 2006. An efficient and economic enhancer mix for PCR. Biochemical and biophysical research communications 347(3), 747-751.

Rao, S.N., Mohan, D.C., Adimurthy, S., 2013. L-proline: an efficient catalyst for transamidation of carboxamides with amines. Organic letters 15(7), 1496-1499.

Tanimoro, K., Ueno, M., Takeda, K., Kirihata, M., Tanimori, S., 2012. Proline catalyzes direct C-H arylations of unactivated arenes. The Journal of organic chemistry 77(18), 7844-7849.

Tarelli, E., Mire-Sluis, A., Tivnann, H.A., Bolgiano, B., Crane, D.T., Gee, C., Lemercinier, X., Athayde, M.L., Sutcliffe, N., Corran, P.H., Rafferty, B., 1998. Recombinant human albumin as a stabilizer for biological materials and for the preparation of international reference reagents.

Biologicals : journal of the International Association of Biological Standardization 26(4), 331-346.

Varadharajan, B., Parani, M., 2021. DMSO and betaine significantly enhance the PCR amplification of ITS2 DNA barcodes from plants. Genome 64(3), 165-171.

Yang, J.W., Chandler, C., Stadler, M., Kampen, D., List, B., 2008. Proline-catalysed Mannich reactions of acetaldehyde. Nature 452(7186), 453-455.

Yin, H., Song, C.Q., Suresh, S., Wu, Q., Walsh, S., Rhym, L.H., Mintzer, E., Bolukbasi, M.F., Zhu, L.J., Kauffman, K., Mou, H., Oberholzer, A., Ding, J., Kwan, S.Y., Bogorad, R.L., Zatsepin, T., Koteliansky, V., Wolfe, S.A., Xue, W., Langer, R., Anderson, D.G., 2017. Structure-guided chemical modification of guide RNA enables potent non-viral in vivo genome editing. Nature biotechnology 35(12), 1179-1187.

Zhang, F., Abudayyeh, O.O., Gootenberg, J.S., 2020. A protocol for detection of COVID-19 using CRISPR diagnostics. https://www.broadinstitute.org/files/publications/special/COVID-19%20detection%20(updated).pdf

Zhang, S., Shen, J., Li, D., Cheng, Y., 2021. Strategies in the delivery of Cas9 ribonucleoprotein for CRISPR/Cas9 genome editing. Theranostics 11(2), 614-648.

Zosel, F., Mercadante, D., Nettels, D., Schuler, B., 2018. A proline switch explains kinetic heterogeneity in a coupled folding and binding reaction. Nature communications 9(1), 3332.

Supplementary Figures

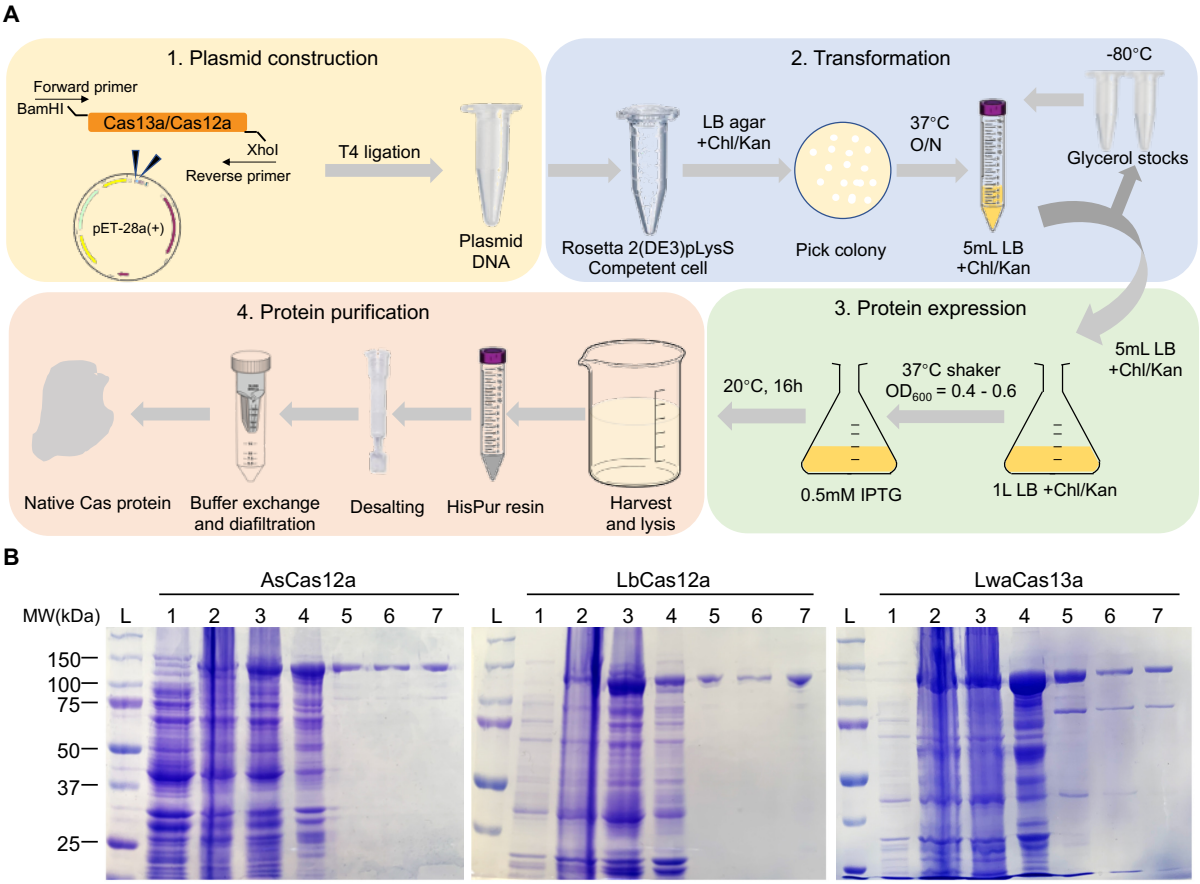

Fig. S1. Expression and purification of Cas protein.

(A) Schematic workflow of protein expression and purification of Cas nucleases.

(B) Different protein fractions collected during protein purification are analyzed by SDS-PAGE and followed by Coomassie Blue staining. L: ladder; 1: non-induced; 2: cell lysate; 3: supernatant of lysate; 4: pellet of lysate; 5: eluted fraction post HisPur Cobalt Resin; 6: fraction post desalting; 7: final purified product post concentrating and buffer exchange.

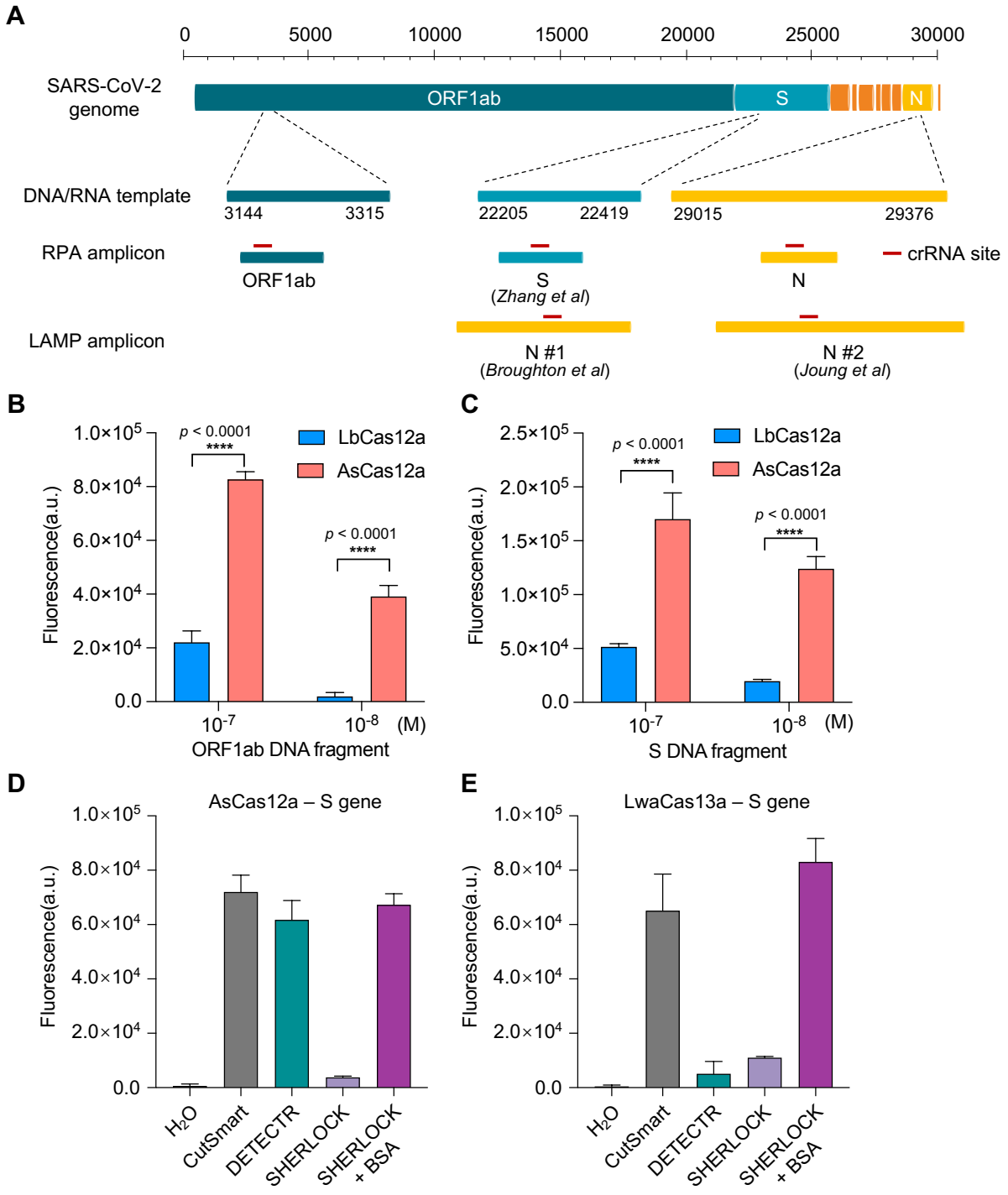

Fig. S2. Schematic of SARS-CoV-2 genome and comparative analysis of trans-cleavage activity between two Cas12a ortholog proteins.

(A) Schematic diagram showing the genomic architecture of SARS-CoV-2 virus. The positions and regions for DNA and RNA templates, RPA and LAMP amplicons, and crRNA-targeting sites used in this study are donated. ORF1ab: open reading frame 1ab; S: spike protein; N: nucleocapsid protein.

(B) Comparison of two Cas12 ortholog proteins (LbCas12a and AsCas12a) for trans-cleavage-mediated detection of synthetic SARS-CoV-2 ORF1ab gene DNA template. Endpoint (60 min)

recording of fluorescence detection signals are shown. Error bars represent mean ± s.d. (n=3). a.u., arbitrary unit. Two-way ANOVA test, ****$p < 0.0001$.
(C) Comparison of two Cas12 ortholog proteins (LbCas12a and AsCas12a) for trans-cleavage-mediated detection of synthetic SARS-CoV-2 S gene DNA template. Endpoint (60 min) recording of fluorescence detection signals are shown. Error bars represent mean ± s.d. (n=3). a.u., arbitrary unit. Two-way ANOVA test, ****$p < 0.0001$.
(D-E) Comparison of different buffers for AsCas12a (D) and LwaCas13a (E) trans-cleavage activity. Buffer sources: DETECTR buffer (NEB2.1) (Broughton et al. 2020); self-prepared custom SHERLOCK buffer (Zhang et al. 2020). Error bars represent mean ± s.d. (n=3). a.u., arbitrary unit.

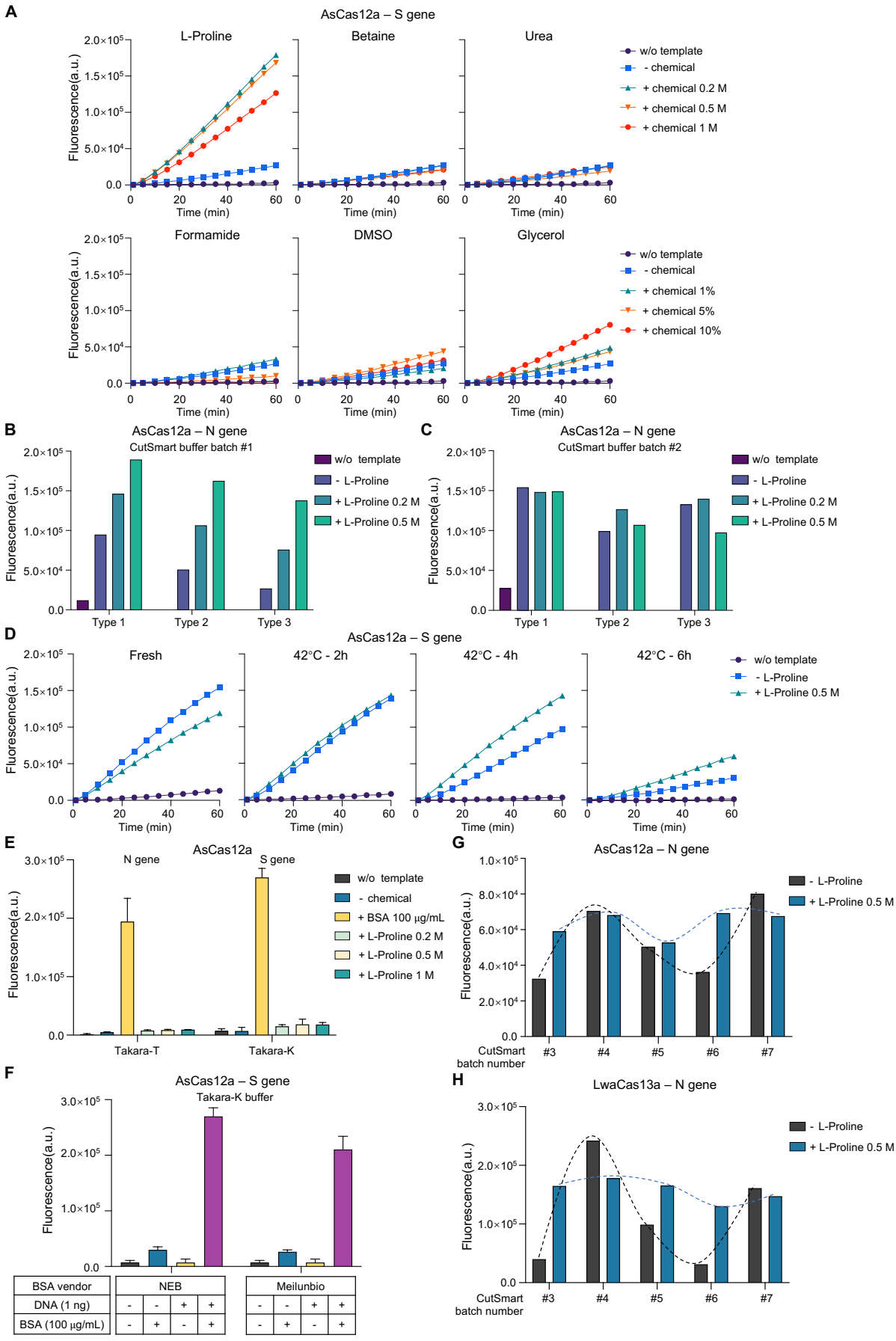
A
AsCas12a – S gene
L-Proline
Betaine
Urea
Formamide
DMSO
Glycerol
Fluorescence(a.u.)
Time (min)
w/o template
- chemical
+ chemical 0.2 M
+ chemical 0.5 M
+ chemical 1 M
+ chemical 1%
+ chemical 5%
+ chemical 10%
B
AsCas12a – N gene
CutSmart buffer batch #1
C
AsCas12a – N gene
CutSmart buffer batch #2
w/o template
- L-Proline
+ L-Proline 0.2 M
+ L-Proline 0.5 M
Type 1
Type 2
Type 3
D
AsCas12a – S gene
Fresh
42°C - 2h
42°C - 4h
42°C - 6h
E
AsCas12a
N gene
S gene
+ BSA 100 µg/mL
+ L-Proline 1 M
Takara-T
Takara-K
F
AsCas12a – S gene
Takara-K buffer
BSA vendor
NEB
Meilunbio
DNA (1 ng)
BSA (100 µg/mL)
G
AsCas12a – N gene
CutSmart batch number
#3
#4
#5
#6
#7
H
LwaCas13a – N gene

Fig. S3. Effects of chemical additives, BSA and buffer batch on CRISPR detection.
(A) Fluorescence signal kinetics of AsCas12a-mediated detection for SARS-CoV-2 S gene synthetic DNA (10^{10} copies) with indicated chemical additives in the reaction mix. w/o template means no input in CRISPR detection system; differential amount of chemicals are added in the reaction mix: no chemical (-), with indicated amount of chemical (+). a.u., arbitrary unit.
(B) Effects of L-proline on AsCas12a-mediated SARS-CoV-2 N gene DNA template detection using different types of Cas protein representing differential states of denaturing in batch #1 CutSmart reaction buffer. L-proline is added in the CRISPR detection mix. Three types of AsCas12a protein are used in this assay - type 1: fresh protein from frozen stock; type 2: protein left at room temperature for 48 hours; and type 3: protein undergone multiple freeze-thaw cycles during 48 hours. Endpoint (60 min) recording of fluorescence detection signals are shown. w/o template means no input in CRISPR detection system; differential amount of L-proline are added in the reaction mix: no L-proline (-), with indicated amount of L-proline (+). a.u., arbitrary unit.
(C) Batch effect of reaction buffers on AsCas12a-based detection and L-proline's enhancement. The same samples used in (B) are gone through the similar assays only except that the reaction buffer changes to batch #2. a.u., arbitrary unit.
(D) Effects of L-proline on AsCas12a-based detection for SARS-CoV-2 S gene DNA template with heat-denatured AsCas12a proteins. AsCas12a protein is pre-heated for 2, 4 and 6 hours in 42°C, and then is examined for their capability on CRISPR detection in the absence (-) or presence (+) of 0.5 M L-proline in the detection mix. Fluorescence signal kinetics is shown. a.u., arbitrary unit.
(E)Effects of BSA and L-proline addition on AsCas12a-mediated SARS-CoV-2 N gene or S gene DNA template detection using Takara-T and Takara-K buffers. Endpoint (60 min) recording of fluorescence detection signals is shown. w/o template means no input in CRISPR detection system; differential amount of chemicals are added in the reaction mix: no chemical (-), with indicated amount of chemical (+). Error bars represent mean ± s.d. (n=3) a.u., arbitrary unit.
(F) Comparison of different sources of BSA on AsCas12a-mediated SARS-CoV-2 N gene DNA template detection in Takara-K buffer. Different vendors of BSA are used. Endpoint (60 min) recording of fluorescence detection signals are shown. Error bars represent mean ± s.d. (n=3) a.u., arbitrary unit.
(G, H) Evaluation of multiple batches (#3 - #7) of CutSmart buffer for the effect on AsCas12a (G) and LwaCas13a (H) detection capability without (-) or with (+) 0.5 M L-proline addition using SARS-CoV-2 N gene DNA (G) or RNA (H) templates. Endpoint (60 min) recording of fluorescence detection signals are shown. a.u., arbitrary unit.

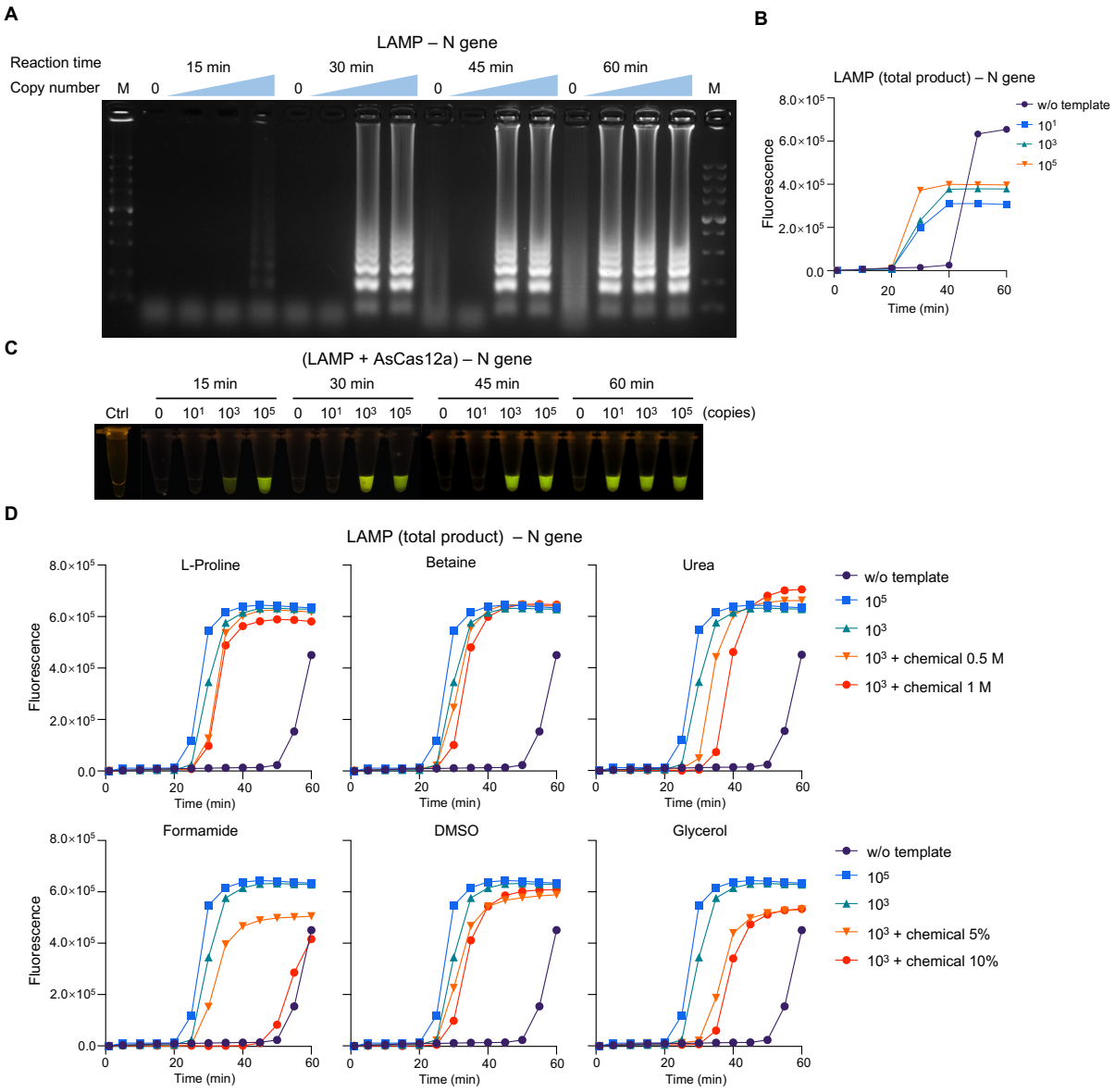

Fig. S4. Evaluation of LAMP and chemical additives for target detection.

(A) Agarose gel electrophoresis of the RT-LAMP products using different amount of SARS-CoV-2 N gene RNA template with different time duration of reactions. LAMP is performed at 62°C for 15, 30, 45 and 60 min. RNA template copy number (left to right): 0, 10^1, 10^3, 10^5 copies.

(B) Dynamic monitoring of total amplification product of RT-LAMP by nonspecific DNA-binding dye EvaGreen using varied amount of SARS-CoV-2 N gene RNA template.

(C) Specific target amplification is determined using purified LAMP products by AsCas12a-based detection with fluorescence signal directly visualized by blue light illuminator. The samples are the same as used in (A).

(D) Evaluation of chemical additives for the effects on total products of RT-LAMP using SARS-CoV-2 N gene RNA template (10^3 and 10^5 copies). Indicated chemicals (+) are added in the LAMP reaction mix and fluorescence kinetics is shown as determined by EvaGreen dye. w/o template means no template input in LAMP reaction.

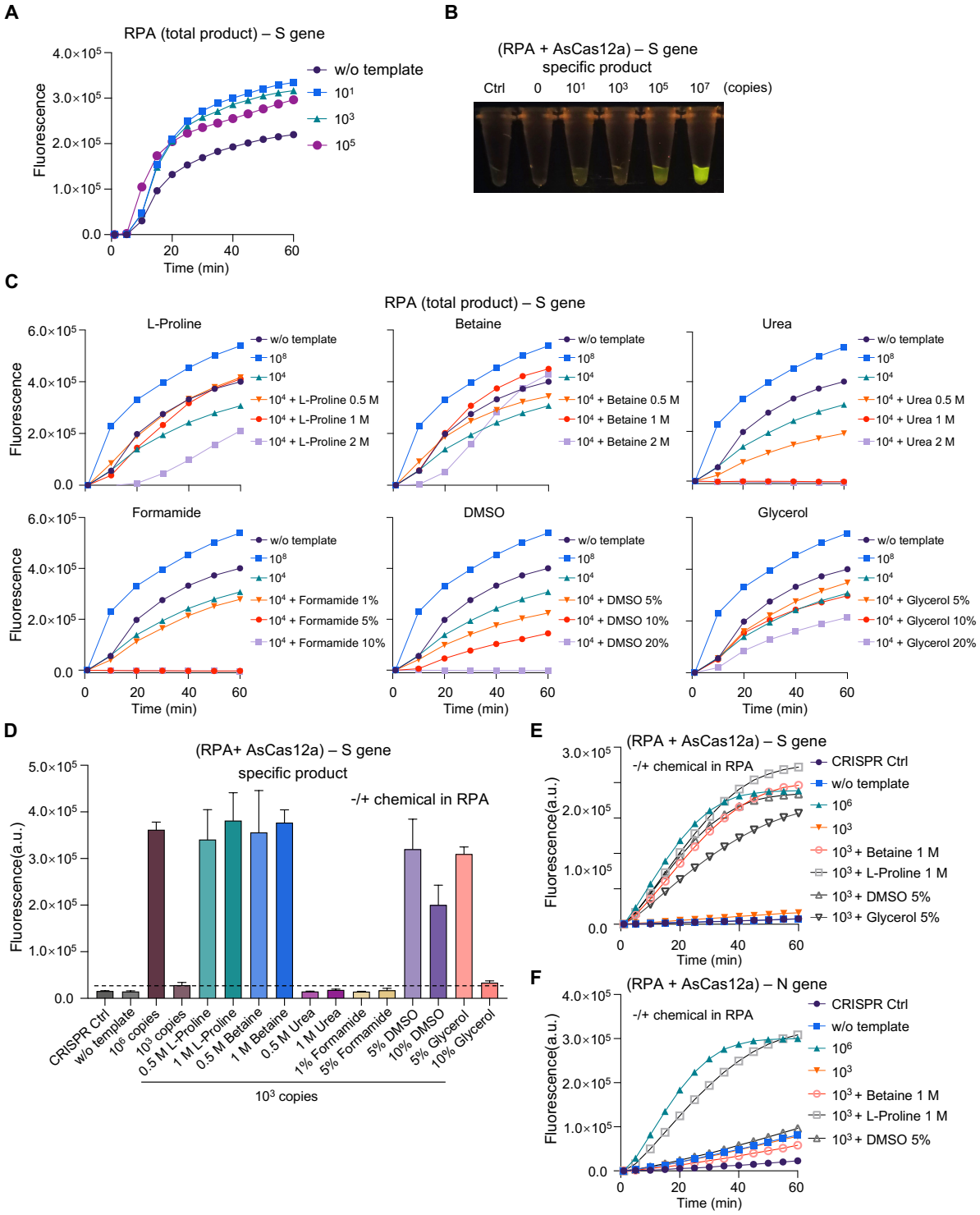

Fig. S5. Evaluation of RPA and chemical additives for target detection.

(A) Dynamic monitoring of total amplification product of RT-RPA by nonspecific DNA-binding dye EvaGreen using varied amount of SARS-CoV-2 S gene RNA template.

(B) Specific target amplification is determined using purified RPA products by AsCas12a-based detection with fluorescence signal directly visualized by blue light illuminator. Varied amount of SARS-CoV-2 S gene RNA templates are used in RT-RPA for a reaction time of 30 min at 40°C before proceeding to purification and CRISPR detection.

(C) Evaluation of chemical additives for the effects on total products of RT-RPA using SARS-CoV-2 S gene RNA template (10^4 and 10^8 copies). Indicated chemicals (+) are added in the RPA reaction mix and fluorescence kinetics is shown as determined by EvaGreen dye. w/o template means no template input in RPA reaction.
(D) Evaluation of different chemical additives for the effect on specific target amplification as determined by AsCas12a-based CRISPR detection using purified RT-RPA products (1:10 dilution) targeting SARS-CoV-2 S gene RNA. Indicated chemicals are included in the RT-RPA reaction mix for a 30 min of reaction at 40°C. The RT-RPA products are purified and then subjected to CRISPR detection. Endpoint (60 min) recording of fluorescence detection signals are shown. The dotted line indicates the fluorescence baseline of CRISPR detection signal from the sample using 10^3 copies of SARS-CoV-2 synthetic RNA template. CRISPR Ctrl indicates no nucleic acid input for AsCas12a detection system; w/o template means no input for RPA reaction. Error bars represent mean ± s.d. (n=3) a.u., arbitrary unit.
(E) Fluorescence kinetics of AsCas12a-based detection is shown for the selected samples used in (D).
(F) Fluorescence kinetics of AsCas12a-based detection are shown to detect specific target amplification from purified RT-RPA products using varied amount of SARS-CoV-2 N gene RNA template in the absence or presence of indicated chemicals. Indicated chemicals are included in the RPA reaction mix for a 30 min of reaction at 40°C. The RPA products are purified and then subjected to CRISPR detection.

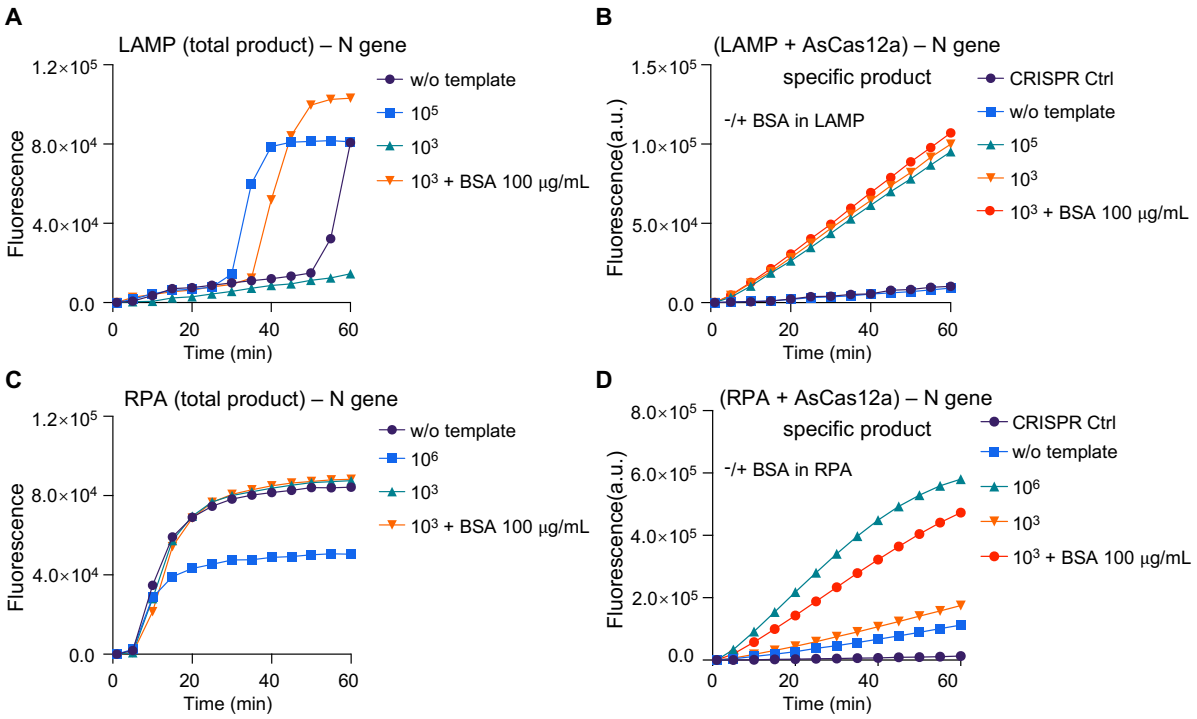

Fig. S6. The effect of BSA on target amplification of LAMP and RPA.

(A) Dynamic monitoring of total amplification product of RT-LAMP by nonspecific DNA-binding dye EvaGreen using varied amount of SARS-CoV-2 N gene RNA template in the absence or presence of BSA. w/o template means no template input in LAMP reaction.

(B) Fluorescence kinetics of AsCas12a-based detection are shown to detect specific target amplification from purified RT-LAMP products (1:50 dilution) using varied amount of SARS-CoV-2 N gene RNA template. BSA is absent or present only in LAMP reaction mix. RT-LAMP reaction is performed for 15 min at 62°C before proceeding to purification and then CRISPR detection. CRISPR Ctrl indicates no nucleic acid input for AsCas12a detection system; w/o template means no input for LAMP reaction.

(C) Dynamic monitoring of total amplification product of RT-RPA by nonspecific DNA-binding dye EvaGreen using varied amount of SARS-CoV-2 N gene RNA template in the absence or presence of BSA. w/o template means no template input in RPA reaction.

(D) Fluorescence kinetics of AsCas12a-based detection are shown to detect specific target amplification from purified RT-RPA products using varied amount of SARS-CoV-2 N gene RNA template. BSA is absent or present only in RPA reaction mix. RT-RPA reaction is performed for 30 min at 40°C before proceeding to purification and then CRISPR detection. CRISPR Ctrl indicates no nucleic acid input for AsCas12a detection system; w/o template means no input for RPA reaction.

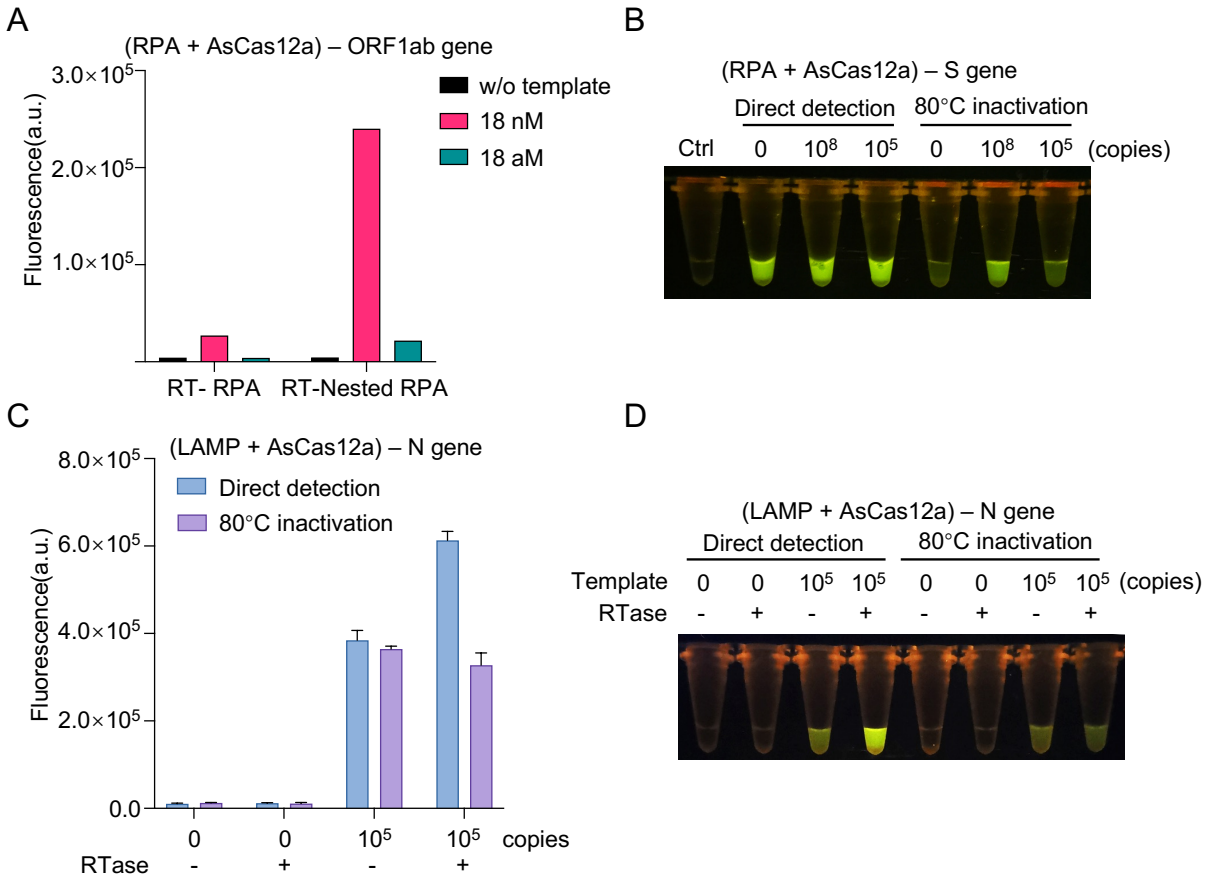

Fig. S7. Performance of RT-Nested RPA and background removal for CRISPR detection.
(A) Comparison of RT-RPA and RT-Nested RPA with varied amount of SARS-CoV-2 ORF1ab gene RNA template. RPA reaction is performed for 10 min at 37°C, and nested RPA has an additional round of pre-amplification for 5 min. 1 μL amplification product is subjected to AsCas12a-based detection and the endpoint (2h) fluorescence signals are shown.
(B) Background signal removal by 80°C heat-inactivation for RPA-AsCas12a two-step detection assays to examine SARS-CoV-2 S gene RNA template. RT-RPA is performed at 40°C for 30 min and 2 μL amplification product is then subjected to AsCas12a-mediated CRISPR detection. Blue light illuminator is used to visualize the endpoint (60 min) fluorescence signal.
(C, D) The effect of reverse transcriptase (RTase) on the background signal of LAMP-AsCas12a-based two-step CRISPR detection system. SARS-CoV-2 N gene DNA template is used for LAMP. The LAMP reaction is performed at 62°C for 15 min and 2 μL amplification product is then subjected to AsCas12a-mediated CRISPR detection. RTase is absent (-) or present (+) only in the CRISPR detection mix. The endpoint (60 min) fluorescence signals are shown by either bar plot (C) or direct visualization under blue light illuminator (D). Error bars represent mean ± s.d. (n=3) a.u., arbitrary unit.

Table S1. The constitutions of different reaction buffers.

Buffer composition	NEBuffer 2	NEBuffer 2.1	NEBuffer 3	NEBuffer 3.1	Takara T	Takara K	Isothermal buffer	CutSmart	SHERLOCK buffer
Magnesium Acetate					10 mM			10 mM	
$MgCl_2$	10 mM	10 mM	10 mM	10 mM		10 mM			6 mM
Potassium Acetate					66 mM			50 mM	
KCl						100 mM	50 mM		
NaCl	50 mM	50 mM	100 mM	100 mM					
Tris-acetate					33 mM			20 mM	
Tris-HCl	10 mM	10 mM	50 mM	50 mM		20 mM	20 mM		40 mM
$(NH_4)_2SO_4$							10 mM		
$MgSO_4$							2 mM		
Tween 20							0.1%		
DTT	1 mM		1 mM		0.5 mM	1 mM			
BSA		100 μg/mL		100 μg/mL				100 μg/mL	
pH	7.9	7.9	7.9	7.9	7.9	8.5	8.8	7.9	7.4

Table S2. Oligonucleotides used in this study.

Primers			
Name	**Sequence (5'–3')**	**Purpose**	**Source**
ORF1ab-PCR (round-1)-F	AGAAGAGCAAGAAGAAGATTGGTTAGATGATGA TAGTCAACAAACTGTTGGTCAACAAGACGGC	Target generation	
ORF1ab-PCR (round-1)-R	AACAATTGTTTGAATAGTAGTTGTCTGATTGTCC TCACTGCCGTCTTGTTGACCAACAG	Target generation	
ORF1ab-PCR (round-2)-F	TGGAATTTGGTGCCACTTCTGCTGCTCTTCAACC TGAAGAAGAGCAAGAAGAAGATTGG	Target generation	
ORF1ab-PCR (round-2)-R	GTAAGTTCCATCTCTAATTGAGGTTGAACCTCAA CAATTGTTTGAATAGTAGTTGTCTG	Target generation	
ORF1ab-PCR-F for IVT	GAAATTAATACGACTCACTATAGGGTGGAATTT GGTGCCACTTCTGCTGC	Target generation	
S-PCR (round-1)-F	GGTAGATTTGCCAATAGGTATTAACATCACTAGG TTTCAAACTTTACTTGCTTTACATAGAAGTTATTT GACTCCTGGTGATTCTTCTTC	Target generation	
S-PCR (round-1)-R	TCCTAGGTTGAAGATAACCCACATAATAAGCTG CAGCACCAGCTGTCCAACCTGAAGAAGAATCAC CAGGAGTCA	Target generation	
S-PCR (round-2)-F	ATCTCCCTCAGGGTTTTTCGGCTTTAGAACCATT GGTAGATTTGCCAATAGGTATTAAC	Target generation	
S-PCR (round-2)-R	GAAAAGTCCTAGGTTGAAGATAACCCACAT	Target generation	

S-PCR (round-3)-F for IVT	GAAATTAATACGACTCACTATAGGGATCTCCCTCAGGGTTTTTCGG	Target generation	
S-PCR (round-3)-R	NNNNNNGGATCCGTAATGGTTCCATTTTCATTATATTTTAATAGAAAAGTCCTAGGTTGAAGATAACCCAC	Target generation	
N #1-PCR-F for IVT	GAAATTAATACGACTCACTATAGGGCAATGTAACACAAGCTTTCGGCAG	Target generation	
N #1-PCR-R	GCGTCAATATGCTTATTCAGCAAAATGAC	Target generation	
N #2-PCR-F	AAGCCTCGGCAAAAACGTACTGCCACTAAAGCATACAATGTAACACAAGCTTTCGGCAG	Target generation	
N #2-PCR-R	GGCTCTGTTGGTGGGAATGTTTTGTATGCGTCAATATGCTTATTCAGCAAAATG	Target generation	
N #2-PCR-F for IVT	GAAATTAATACGACTCACTATAGGGAAGAAATCTGCTGCTGAGGCTTCTAAGAAGCCTCGGCAAAAACGTAC	Target generation	
ORF1ab-AsCas12a-crRNA	GGTTAGATGATGATAGTCAAATCTACAAGAGTAGAAATTACCCTATAGTGAGTCGTATTAATTTC	crRNA generation	
ORF1ab-LbCas12a-crRNA	GGTTAGATGATGATAGTCAAATCTACACTTAGTAGAAATTACCCTATAGTGAGTCGTATTAATTTC	crRNA generation	
S-AsCas12a-crRNA	GAAGAAGAATCACCAGGAGTATCTACAAGAGTAGAAATTACCCTATAGTGAGTCGTATTAATTTC	crRNA generation	
S-LbCas12a-crRNA	GAAGAAGAATCACCAGGAGTATCTACACTTAGTAGAAATTACCCTATAGTGAGTCGTATTAATTTC	crRNA generation	
S-LwaCas13a-crRNA	ACTCCTGGTGATTCTTCTTCAGGTTGGAGTTTTAGTCCCCTTCGTTTTTGGGGTAGTCTAAATCCCCTATAGTGAGTCGTATTAATTTC	crRNA generation	
N #1-AsCas12a-crRNA	GAACGCTGAAGCGCTGGGGGATCTACAAGAGTAGAAATTACCCTATAGTGAGTCGTATTAATTTC	crRNA generation	
N #2-AsCas12a-crRNA	CTGATTACAAACATTGGCCGATCTACAAGAGTAGAAATTACCCTATAGTGAGTCGTATTAATTTC	crRNA generation	
N-LwaCas13a-crRNA	ACAATTTGCCCCCAGCGCTTCAGCGTTCGTTTTAGTCCCCTTCGTTTTTGGGGTAGTCTAAATCCCCTATAGTGAGTCGTATTAATTTC	crRNA generation	
T7-F	GAAATTAATACGACTCACTATAGGG	IVT	Kellner et al., 2019
N #1-F3	AACACAAGCTTTCGGCAG	LAMP	Broughton et al., 2020
N #1-B3	GAAATTTGGATCTTTGTCATCC	LAMP	Broughton et al., 2020
N #1-BIP	TGCGGCCAATGTTTGTAATCAGCCAAGGAAATTTTGGGGAC	LAMP	Broughton et al., 2020

N #1-FIP	CGCATTGGCATGGAAGTCACTTTGATGGCACCTGTGTAG	LAMP	Broughton et al., 2020
N #1-LF	TTCCTTGTCTGATTAGTTC	LAMP	Broughton et al., 2020
N #1-LB	ACCTTCGGGAACGTGGTT	LAMP	Broughton et al., 2020
N #2-F3	GCTGCTGAGGCTTCTAAG	LAMP	Joung et al., 2020
N #2-B3	GCGTCAATATGCTTATTCAGC	LAMP	Joung et al., 2020
N #2-BIP	TCAGCGTTCTTCGGAATGTCGCTGTGTAGGTCAACCACG	LAMP	Joung et al., 2020
N #2-FIP	GCGGCCAATGTTTGTAATCAGTAGACGTGGTCCAGAACAA	LAMP	Joung et al., 2020
N #2-LF	CCTTGTCTGATTAGTTCCTGGT	LAMP	Joung et al., 2020
N #2-LB	TGGCATGGAAGTCACACC	LAMP	Joung et al., 2020
ORF1ab-RPA-Outer-F	GAAATTAATACGACTCACTATAGGGTCTTCAACCTGAAGAAGAGCAAGAA	RPA	
ORF1ab-RPA-Outer-R	CAATTGTTTGAATAGTAGTTGTCTGATTGTCCTCA	RPA	
ORF1ab-RPA-Inner-F	GAAATTAATACGACTCACTATAGGGTGGAATTTGGTGCCACTTCTGCTGC	RPA	
ORF1ab-RPA -Inner-R	GTAAGTTCCATCTCTAATTGAGGTTGAACCTC	RPA	
S-RPA-F	AGGTTTCAAACTTTACTTGCTTTACATAGA	RPA	https://www.broadinstitute.org/files/publications/special/COVID-19%20detection%20(updated).pdf
S-RPA-R	TCCTAGGTTGAAGATAACCCACATAATAAG	RPA	https://www.broadinstitute.org/files/publications/special/COVID-19%20detec

			tion%20(updated).pdf
N-RPA-F	TGATTACAAACATTGGCCGCAAATTGCACA	RPA	
N-RPA-R	ACGTTCCCGAAGGTGTGACTTCCATGCCAA	RPA	
N #2-PCR-F	CTTGGTACCAAGAAATCTGCTGCTGAGGCTTC	Plasmid construction	
N #2-PCR-R	CCACAGGATCCGCGTCAATATGCTTATTCAGCAAAATGAC	Plasmid construction	
Synthesized dsDNA gene fragment			
Name	**Sequence (5'–3')**		
N #1	GTCTGTACTGCCGTTGCCACATAGATCATCCAAATCCTAAAGGATTTTGTGACTTAAAAGGTAAGTATGTACAAATACCTACAACTTGTGCTAATGACCCTGTGGGTTTTACACTTAAAAACACAGTCTGTACCGTCTGCGGTATGTGGAAAGGTTATGGCTGTAGTTGTGATCAACTCCGCGAACCCATGCTTCAGTCAGCTGATGCACAATCGTTTTTAAACGGGTTTGCGGTGTAAGTGCAGCCCGTCTTACACCGTGCGGCACAGGCACTAGTACTGATGTCGT	DNA target	
Reporters			
Name	**Sequence (5'–3')**	**Purpose**	**Source**
Cas12a FQ-reporter	/56-FAM/TTATT/3BHQ_1/	Fluorescent	Modified from Chen et al., 2018
Cas12a LF-reporter	/56-FAM/TTATTATT/3Bio/	Lateral flow	Broughton et al., 2020
Cas13a FQ-reporter	/56-FAM/rUrUrUrUrU/3BHQ_1/	Fluorescent	Modified from Kellner et al., 2019

Table S3. Reagents and instruments used in this study.

Reagent/Instrument name	Commercial vendor	Item No.
10x T buffer	Takara Bio	SD6092
10x K buffer	Takara Bio	SD0008
10x Isothermal Amplification Buffer	New England Biolab® Inc	B0374S
CutSmart® Buffer	New England Biolab® Inc	B7204S
NEBuffer™ 2	New England Biolab® Inc	B7002S
NEBuffer™ 2.1	New England Biolab® Inc	B7202S
NEBuffer™ 3	New England Biolab® Inc	B7003S

NEBuffer™ 3.1	New England Biolab® Inc	B7203S
Bst 2.0 WarmStart DNA Polymerase	New England Biolab® Inc	M0538S
Phanta Max Super-Fidelity DNA Polymerase	Vazyme	P505
WarmStart RTx Reverse Transcriptase	New England Biolab® Inc	M0380S
NxGen® T7 RNA polymerase	Lucigen	30223-1
ProtoScript II Reverse Transcriptase	New England Biolab® Inc	M0368S
High-Capacity cDNA Reverse Transcription Kit	Thermo Fisher	4368813
T4 DNA ligase	Thermo Fisher	EL0016
RNaseOUT™ Recombinant Ribonuclease Inhibitor	Thermo Fisher	10777019
BamH I restriction enzyme	Takara Bio	1010A
Kpn I restriction enzyme	Takara Bio	1068A
Xho I restriction enzyme	Takara Bio	1094B
Rosetta 2(DE3)pLySs	Youbio	ST1147
Isopropyl β-D-thiogalactoside	Sorlabio	I8070
Lysozyme	Solarbio	L8120
PMSF	Beyotime	ST505
BCA protein assay kit with BSA	Meilunbio	MA0082
HisPur™ Cobalt Resin	Thermo Fisher	89964
Zeba™ Spin Desalting Columns, 7K MWCO, 2 mL	Thermo Fisher	89889
Amicon® Ultra-15 Centrifugal Filter Unit	Milipore	UFC905008
Lipofectamine™ 2000 Transfection Reagent	Thermo Fisher	11668019
Opti-MEM™, Reduced Serum Medium, no phenol red	Thermo Fisher	11058021
L-Proline	Solarbio	SP8540
Betaine	Solarbio	B8230
Urea	Solarbio	U8020
Formamide	Sigma Aldrich	F9037
Dimethyl sulfoxide	Solarbio	D8370
Glycerol	Sangon Biotech	A600232
Bovine serum albumin	New England Biolab® Inc	B9000S
qPCR Lentivirus Titer Kit	Applied Biological Materials Inc	LV900
RNA Clean & Concentrator™-5	ZYMO RESEARCH	R1013
GeneJET PCR Purification Kit	Thermo Fisher	K0702
TwistAmp® Basic	TwistDx™	tabas03kit
EvaGreen® Dye, 20x in Water	Biotium	31000
HybriDetect-Universal Lateral Flow Assay Kit	Milenia Biotec GmbH	MGHD 1
UltraPure™ DNase/RNase-Free Distilled Water	Thermo Fisher	10977015
E-Gel™ Safe Imager™ Real-Time Transilluminator	Thermo Fisher	G6500
Qubit® 3.0 Fluorometer	Thermo Fisher	Q33216
QuantStudio™ 5 Real-Time PCR System	Thermo Fisher	A28139
Ultrasonic cell disruptor	Ningbo Scientz Biotechnology	II D

Novel Coronavirus (2019-nCoV) Dual Probes qRT-PCR Kit	Beyotime	D8006S
COVID-19 (Corona Virus Disease 2019) RNA Reference material（high concentration）	National Institute of Metrology, China	GBW(E)091089